Resolution of fluorescence intensity decays of the two tryptophan residues in glutamine-binding protein from *Escherichia coli* using single tryptophan mutants

P. H. Axelsen,* Z. Bajzer,* F. G. Prendergast,* P. F. Cottam‡ and C. Ho‡
*Department of Biochemistry and Molecular Biology, Mayo Clinic and Foundation, Rochester, Minnesota 55905; and
‡Department of Biological Sciences, Carnegie Mellon University, Pittsburgh, PA 15213 USA

ABSTRACT Time correlated single photon counting measurements of tryptophan (Trp) fluorescence intensity decay and other spectroscopic studies were performed on glutamine-binding protein (GlnBP) from *Escherichia coli*. Using site-specifically mutated forms of the protein in which tryosine (Tyr) and phenylalanine (Phe) substitute for the Trp residues at positions 32 and 220, we have examined whether wild-type (Wtyp) intensity decay components may be assigned to specific Trp residues. Results indicate that: (*a*) two exponential intensity decay components are recovered from the Wtyp protein (6.16 ns, 0.46 ns); (*b*) the long decay component arises from Trp-220 and comprises >90% of the total fluorescence emission; (*c*) the short component arises from Trp-32 and is highly quenched; (*d*) all four single-Trp mutants exhibit multiexponential intensity decays, yet equimolar mixtures of two single-Trp mutants yield only two decay components which are virtually indistinguishable from the Wtyp protein; (*e*) the recovery of additional components in protein mixtures is obscured by statistical noise inherent in the technique of photon counting; (*f*) various spectroscopic measurements suggest that Trp–Trp interactions occur in the Wtyp protein, but the Wtyp intensity decay may be closely approximated by a linear combination of intensity decays from single-Trp mutants; and (*g*) inferences derived independently from fluorescence and NMR spectroscopy which pertain to the presence of Trp–Trp interactions and the relative solvent exposure of the two Trp residues are in agreement.

INTRODUCTION

Protein fluorescence is exquisitely sensitive to changes in the physico-chemical environment of protein fluorophores. Unfortunately, our ability to interpret these changes in protein fluorescence in terms of protein structure lags far behind our ability to detect changes. The interpretation of Trp fluorescence in proteins is especially problematic when attempting to study proteins containing two or more Trp residues. Various means have been described for resolving residue-specific fluorescence signals in a multi-Trp protein (1–5), but in general, these approaches depend on our ability to resolve discrete exponential components in the fluorescence intensity decay. Resolving exponential components in such decays is analogous to the problem of resolving individual signals in a mixture of fluorophores. However, this type of analysis is a nontrivial problem and may be further complicated in proteins by Trp–Trp interactions.

Site-specific mutation of Trp residues to yield single-Trp forms of a multi-Trp containing protein is an obvious approach to the problem, but is subject to pitfalls because there is no structurally or photophysically "conservative" substitution for Trp. It is incumbent on the investigator to show that substitution has not altered the structure of a protein, i.e., that the Trp environment in the mutant form faithfully preserves the environment of the corresponding Trp in the wild-type protein. Another problem is inherent in analysis of time-resolved results: it is not straightforward to determine whether a specific decay component has been altered simply by removal of an electronically active species in the vicinity (e.g., Trp), or whether the data fitting procedure is simply unable to firmly resolve a particular decay component in the presence of additional components.

We have examined the fluorescence intensity decay characteristics of glutamine-binding protein (GlnBP) from *E. coli*, a 256 residue monomeric protein with Trp residues at positions 32 and 220, and four mutant forms of GlnBP prepared by site-specific mutagenesis (Tyr and Phe substitutions for each Trp [6]). Earlier NMR investigations of these five proteins indicated that the wild-type protein conformation is preserved in spite of the substitutions. In addition, proteins prepared with 6-^{19}F-Trp, indicate that the two Trp residues are sensitive to bound L-glutamine (Gln) and to each other: the binding of Gln shifts both ^{19}F resonances in the wild-type protein, but has no effect on the single-Trp mutants (6).

We have studied this system to ask whether fluorescence intensity decay measurements on the wild-type

Correspondence should be addressed to Dr. P. H. Axelsen.
Dr. Ž. Bajzer is on leave of absence from Rudjer Bošković Institute, Zagreb, Croatia, Yugoslavia.

0006-3495/91/09/650/10 $2.00

protein may be resolved into the same components found in single-Trp forms. In an earlier study of *lac* repressor protein and two single Trp mutants, Royer et al. (7) found that the wild-type intensity decay corresponded to the weighted linear combination of decays from the single-Trp mutant proteins. We have taken a similar approach to the study of GlnBP, but have also examined the sensitivity of linear combination analysis, and whether photophysical interactions occurring between Trp residues (as suggested by NMR studies) may be demonstrated by this approach. We have also examined whether there is agreement between other inferences derived independently from NMR and fluorescence studies of GlnBP.

METHODS

GlnBP (Wtyp) and site-specific mutants (W32Y, W32F, W220Y, and W220F) were prepared as described previously (6) and used at a concentration of ~20 μM in 10mM-phosphate buffer at pH 7. Spectra and intensity measurements were made a spectrofluorometer (model MPF-66, Perkin Elmer Corp., Norwalk, CT) using a 150-Watt xenon lamp and Rhodamine 101 quantum counter. All spectra had background intensities subtracted and were corrected for lamp and monochromator variations. Absorption spectra were measured on a CARY 2200 spectrophotometer with a 0.5-nm slit width. Molar quantum yields were determined relative to Trp in water (taken to be 0.14 [8]) using the relationship

$$\frac{\Phi_{prot}}{\Phi_{Trp}} = \frac{\int I_{prot}}{\int I_{Trp}} \frac{A_{Trp}}{A_{prot}},$$

where Φ is quantum yield, $\int I$ is the integrated intensity over the emission wavelength range 300–400 nm, and A is the absorbance at 295 nm. Subscripts prot and Trp refer to protein and Trp, respectively. Protein concentration was determined by quantitative amino acid analysis for a sample of Wtyp protein which was purified as described by Shen et al. (9). The concentrations of the mutated proteins relative to Wtyp was then determined by a bicinchoninic acid-based assay (Microtiter Plate BCA assay, Pierce Chemical Co., Rockford, IL) assuming a molecular weight of 25,000. "Molar" quantum yields were determined from above equation by substituting molar absorptivity for absorbance in anticipation of studies on equimolar mixtures of single-Trp mutants.

Time-resolved fluorescence intensity decay measurements were performed by time-correlated single photon counting (TCSPC) on a laser-based fluorometer similar to that described previously (10). The instrument response function FWHM was approximately 40 ps, and a channel width of 27.8 ps was used. Multiple measurements imply recordings collected on separate days. The instrument response function (IRF) and decay function were both counted until 20,000 counts were collected in the peak channel. Excitation at 295 nm produces Raman scatter centered at 327 nm. Therefore, intensity decays were recorded at 317, 337, and 357 nm to avoid this contribution.

The data were fit with model functions generated by convolving the instrument response function with an n-component decay function (11). The latter is the sum of n exponential terms (components) each of which is characterized by parameters representing lifetime and fractional intensity (i.e., not a preexponential factor). In addition, the model function incorporates a time-shift parameter yielding a total of $2n + 1$ parameters for each model function. A simplex method (12) is used to adjust model parameters and minimize the chi-squared deviance between the predicted decay function and the experimental dataset. In the procedure developed for this work, up to 10 model functions and datasets may be fit simultaneously, in which case the overall chi-squared statistic is minimized. While fitting data simultaneously, various constraints may be applied to the model parameters. For example, parameters in different model functions (each function being fit to a different set of data) may be constrained to be equal, i.e., "linked." Alternatively, the ratio between two parameters in one model function may be linked to the ratio of two parameters in another model function. Parameters may also be assigned fixed values. Double-precision (8-byte) precision is used throughout the fitting procedure.

Single-decay functions were also analyzed using the global analysis software package, Globals Unlimited (University of Illinois, Urbana, IL.) (13–16). However, this software does not normalize fractional intensities for time-domain analyses. Thus, parameter linkages involving fractional intensities as described above are not possible. With respect to discrete lifetime analysis, we have used this software primarily to verify the results of our own procedure. This software was also used for fitting lifetime distributions to individual datasets.

To decide the number of components to be used in a model function, the χ^2 deviance corresponding to a 95% confidence level was determined for the fractional intensity of a component by means of an F-statistic (17). For a given number of degrees of freedom, the F-statistic describes the probability that the ratio of two deviances will not exceed a given value. Thus, the confidence interval for a selected parameter is defined by varying the value of a selected parameter across a desired range, and fitting the model function to the data with this parameter value fixed. The deviances thus obtained are compared to the overall minimum deviance, and the point at which the deviance ratio exceeds that described by the F-statistic marks a limit of the confidence interval. If the fractional intensity of any component could be fixed at zero without exceeding the specified deviance ratio, the component was rejected.

RESULTS

Fluorescence emission spectra and quantum yields

The Trp fluorescence emission spectra for the Wtyp and mutant proteins at λ_{ex} = 295 nm are smooth and featureless. The emission maximum is 330 nm for the Wtyp, W32Y, and W32F proteins. W220F is relatively blue shifted to 326 nm, and W220Y is shifted even further to 316 nm. These data are comparable to that of Weiner and Heppel (18) who recorded an emission maximum of 336 nm with excitation at 280 nm. These authors reported a blue shift upon binding Gln. We find that 400 μM Gln (20–40 μM protein) causes a 1.5-nm blue shift in Wtyp, 1.0-nm blue shifts in W32Y, W32F, and W220Y, and a 1.0-nm red shift in W220F. The results are unchanged if excitation at 300 nm is used.

The quantum yields relative to Trp in water (=0.14) at λ_{ex} = 295 nm over the range 300–400 nm are given in Table 1. The quantum yields of W32Y and W32F are

TABLE 1 **Molar absorptivities, quantum yield, molar quantum yield, and emission maxima of GlnBP and single Trp mutants**

Portein	ϵ	Q.Y.	Q.Y. (molar)	λ_{max}
Wtyp	7100	0.22	0.23	330
W32Y	4700	0.28	0.30	330
W32F	5100	0.30	0.31	330
W220Y	4100	0.024	0.012	316
W220F	4100	0.043	0.022	326
Trp	1500	0.14	0.14	352

The dimension of ϵ is molar^{-1} cm^{-1}, and λ_{max} is nanometers. Values for Trp in pH7 buffer are given for reference (ϵ and λ_{max} are measured values).

greater than that of Wtyp, whereas W220F is considerably lower, and W220Y is even lower. Thus, the protein with the most blue-shifted emission also exhibits the lowest quantum yield. The addition of Gln caused a slight decrease in the quantum yield of all five proteins (data not shown). Second derivative absorption spectra (Fig. 1) reveal a small shoulder (i.e., negative second derivative) at 293 nm in the Wtyp and W220X proteins which is absent in W32X mutants.

Fluorescence intensity decay

The intensity decay components recovered from the analysis of TCSPC data is reported in Table 2. In almost all cases, the model fits the data significantly better when a small "scatter component" is included. We have not reported parameters for components with lifetimes less than two channel widths (i.e., <55 ps) and fractional intensities <1%.

The Wtyp protein exhibits an apparent biexponential decay with a 6.16-ns component, comprising a progressively larger fraction of the decay with increasing wavelength. 95% confidence ranges for the Wtyp components are 6.10–6.22 ns (τ_1) and 0.41–0.52 ns (τ_2). Two components were also recovered from W32Y and W32F, although the shorter of the components have small fractional intensities. The major component of W32Y is 6.13 ns which corresponds well to the 6.16-ns component of the Wtyp protein. The major component of W32F is slightly longer (6.35 ns). Three components are recovered from W220Y and W220F with a 0.4–0.5 ns component in these proteins corresponding most closely to the second Wtyp component. However, the fractional inten-

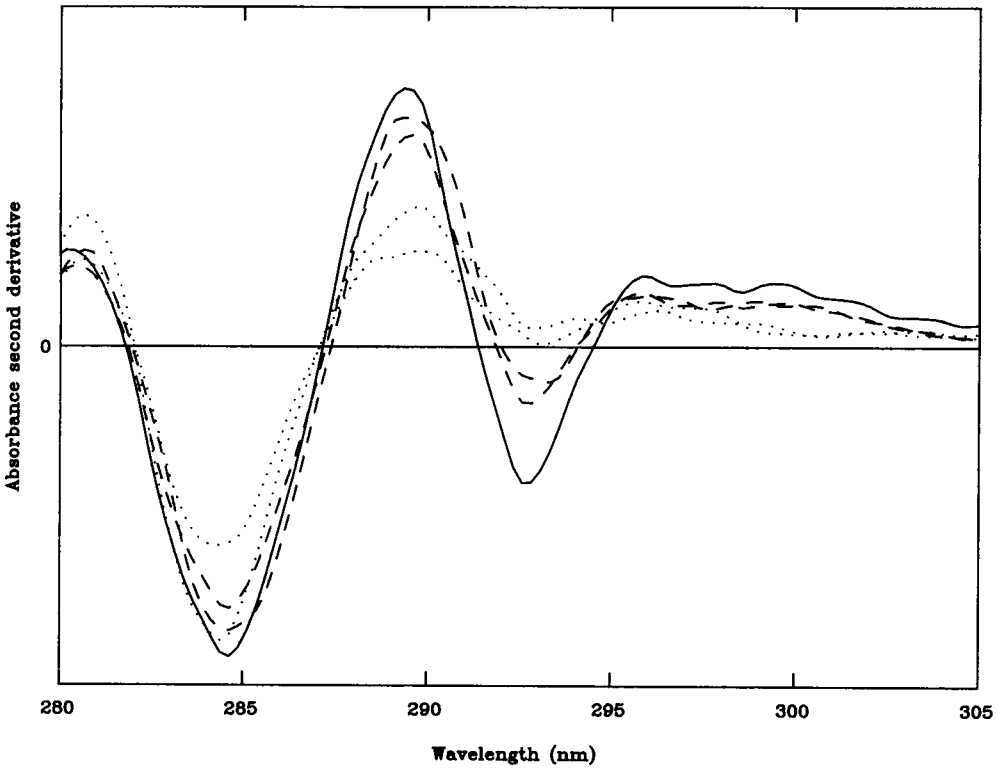

FIGURE 1 Second derivative absorbance spectra of Wtyp GlnBP (*solid line*) and four single-Trp mutants (W32X: *dotted lines*, W220X: *dashed lines*). Protein concentrations were adjusted to 20.0 μM for each measurement.

TABLE 2 **Flourescence intensity decay results for wild-type GLN-BP and four mutants**

Protein	λ_{em}	n	τ_1	f_1	τ_2	f_2	τ_3	f_3	χ^2
WTYP	317	3		.913		.082			
	337	3	6.16 (6.10–6.22)	.959	.46 (.41–.52)	.039			1.70
	357	3		.974		.025			
W32-Y	317	2		.979		.019			
	337	2	6.13 (6.06–6.20)	.991	.74 (.47–1.16)	.009			1.73
	357	2		.994		.006			
W32-F	317	2		.984		.014			
	337	2	6.35 (6.30–6.41)	.997	1.51 (.50–4.80)	.001			1.87
	357	2		.999		.000			
W220-Y	317	2		.217		.754		.029	
	337	2	4.01 (3.81–5.06)	.196	.53 (.51–1.75)	.785	.07 (.02–.48)	.019	1.75
	357	2		.231		.758		.011	
W220-F	317	2		.394		.123		.473	
	337	2	5.50 (5.14–12.37)	.517	1.75 (.77–3.94)	.117	.44 (.36–.47)	.357	1.57
	357	2		.609		.112		.270	
YY	317	2		.897		.098		.066	
	337	3	6.17 (6.09–6.25)	.953	.59 (.51–.75)	.045	.08 (.01–.33)	.002	1.93
	357	2		.973		.027		.000	
YF	317	2		.901		.093			
	337	3	6.16 (6.11–6.23)	.955	.54 (.48–.64)	.043			1.58
	357	2		.973		.027			
FY	317	2		.903		.097			
	337	3	6.32 (6.26–6.39)	.959	.51 (.46–.56)	.041			1.87
	357	2		.977		.023			
FF	317	2		.907		.089			
	337	3	6.30 (6.23–6.38)	.959	.51 (.45–.61)	.039			1.73
	357	2		.977		.023			

For each protein, a simultaneous fit was made with lifetimes linked across all 3 emission wavelengths (λ_{em}) and fractional intensities linked across the measurements made at a single wavelength. A 95% confidence interval is given in parentheses for selected lifetimes. The number of measurements (n) indicates how many measurements (each made on a different day) were fit simultaneously for each wavelength. If we could not exclude a component at any one of the three wavelengths by the criteria given above in Methods, the component was fit at all three wavelengths regardless of whether the component could be excluded at other wavelengths. A component with a very short lifetime (< 0.055 ns) was almost always necessary to achieve the quality of fit reported here, and could not be excluded by our criteria. However, components are only listed in this table if their lifetime was > 0.055 ns (i.e., two channel widths) or if their fractional intensity was $\geq 1\%$.

sities of all components vary with emission wavelength, suggesting heterogeneous origins.

Compared to the discrete exponential model, we were unable to improve the quality of fit for W220Y and W220F by the use of lifetime distributions (Gaussian and Lorentzian) and the same or fewer parameters. The effect of 400 μM Gln was more or less uniform in all five proteins: the longest component in each case was shortened by 0.3–0.5 ns, whereas the next longest component was virtually unchanged (data not shown).

Equimolar (1:1) mixtures of the single Trp mutants were also examined (YY, YF, FY, FF: first letter = position 32, substituted, second letter = position 220, substituted). The first component of the FY and FF mixtures (Table 2) is longer than that of YY and YF mixtures, a relationship matched by the longer first component of W32F relative to that of W32Y. The first component in each mixture also exhibits a greater fractional intensity at longer wavelengths, as seen in the Wtyp protein. A 0.51–0.59-ns component is recovered from each mixture, apparently corresponding to the second component of the Wtyp protein and the W220X mutants.

If only the data collected at 337 nm are analyzed simultaneously, two components are recovered, χ^2 ranges from 1.5–1.8, and the components recovered (not shown) are very similar to those recovered when data from all three wavelengths are used (Table 2). In such analyses (on 337-nm data), we have added parameters with fixed values corresponding to those components recovered in

the individual mutant proteins but missing in the protein mixtures. In general, this can be done without increasing χ^2 by more than 0.01, i.e., the χ^2 surface with respect to these parameters is virtually flat. If they had emerged as solutions, these components would have been excluded by the criterion given above.

Simulations

To examine whether it is theoretically possible to recover the components from different proteins in a mixture, we have conducted simulations using the four individual components found for W32Y and W220Y as input parameters. A typical instrument response function with ~20,000 counts in the peak channel was convolved with a model function comprised of the four exponential components, and Poisson noise was added. This was repeated to yield 100 different sample decay functions and each of the decay functions were fit to model functions of three or four components in the manner done for "real" data. The results are given in Fig. 2 as plots of recovered lifetime vs. fractional intensity/lifetime. In this case, input lifetimes (fractional intensities) were taken from two-component fits to data recorded at 337 nm, namely 6.14 ns (0.934) and 0.96 ns (0.009) for W32Y, and 4.03 ns (0.011) and 0.52 ns (0.044) for W220Y (at 337 nm, the third component given in Table 2 for W220Y is not recovered). The fractional intensities were scaled according to a relative quantum yield of 0.04 for the W220Y components.

Fig. 2 shows that the components actually recovered from this simulated decay function cluster around only two lifetimes. In some cases, the 0.96 component appears to be recovered at an appropriate fractional intensity, but there are essentially no recoveries of the 4.03-ns component. The recovered values clearly resemble Lorentzian distributions about two different lifetimes. However, we must emphasize that these are distributions of fitted parameter values, *not* distributions of lifetimes as are hypothesized to exist in proteins (19). The input data to these simulations were discrete lifetimes, and the distributions arise solely as a result of statistical noise.

Linked analyses with mutant proteins

The decay function recorded from a mixture of two proteins should be a linear sum of the individual decay functions. Therefore, we have attempted to recover the components recovered from single-Trp mutants in an equimolar mixtures of single-Trp mutants using linked simultaneous (i.e., "global") analysis. This analysis ad-

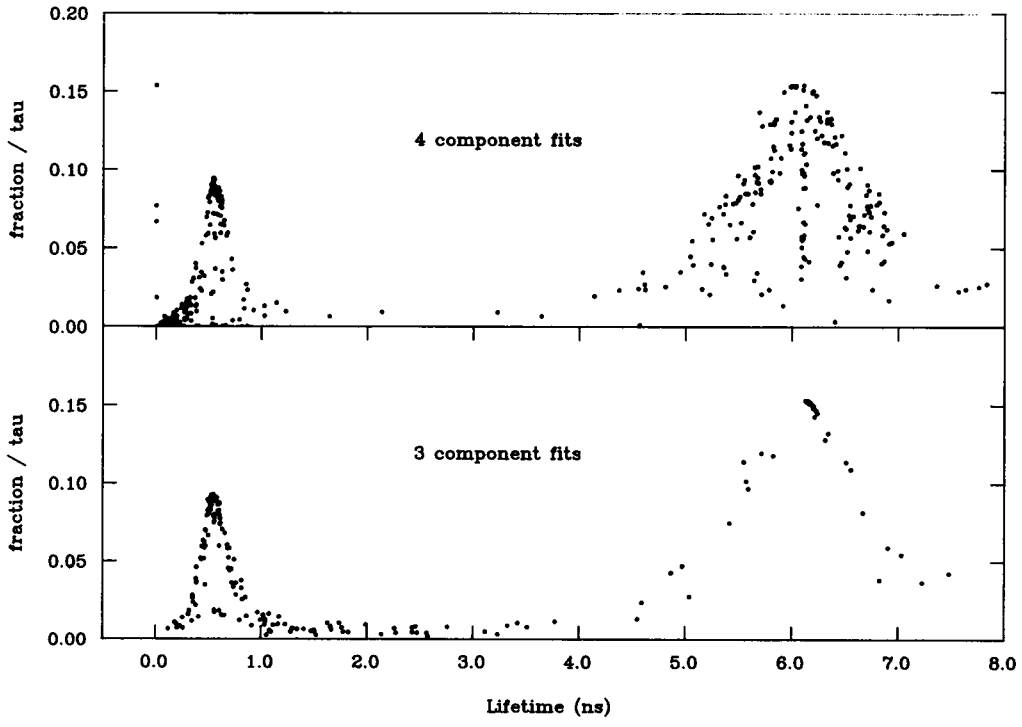

FIGURE 2 Recovered parameters for three- and four-component fits in 100 simulated experiments. Input parameters for the simulations are given in the text.

dresses two questions: (*a*) Does the intensity decay function of a protein mixture remain a linear combination of the individual proteins in spite of the aforementioned statistical noise? (*b*) Is the intensity decay behavior of individual Trp residues in the Wtyp protein altered from the decay exhibited in the single Trp mutants? If so, the Wtyp intensity decay should not be a linear sum of the mutant decay functions.

When attempting to simultaneously fit the intensity decays from two single Trp mutants along with the Wtyp protein an equimolar mixture of single-Trp mutants, a complex system of parameter linkages is necessary to assure that the recovered parameters will have meaningful relationships. The parameters reported in Table 3 *a* were recovered by linking lifetimes τ_1 and τ_4 between the W32Y mutant and an equimolar mixture of the W32Y and W220Y mutants. Likewise, τ_2 and τ_3 were linked between W220Y and the mixture. The ratios of f_2:f_3 and f_1:f_4 were linked, and both parameters of the fifth component were linked across all three measurements. These constraints alone yielded an excellent fit (overall $\chi^2 = 1.4$), but only at the expense of setting both f_2 and f_3 to zero. It was necessary to constrain the sum of $f_2 + f_3$ to 0.037 (corresponding to the relative molar quantum yield of W220Y versus W32Y) to achieve a meaningful simultaneous fit. It was hoped that this constraint would not be necessary, so that the sum of $f_2 + f_3$ could be compared to the relative quantum yield of the two proteins and thus serve as an internal check on our interpretation of these components. Apparently, the fitting routine cannot recover these components because it cannot identify a local minimum in the intensity decay of the mixture (cf the virtually flat χ^2 surface observed when additional components were added in the course of fitting data from equimolar mixtures, as noted above).

Surprisingly, analysis of the Wtyp protein in this manner yielded a significantly better fit than mutant protein mixtures in two out of three measurements (Table 3 *b*). This seems to indicate that the intensity decay of the Wtyp protein can be recovered as a linear combination of single-Trp proteins decays. However, we did not allow the sums $f_1 + f_4$ and $f_2 + f_3$ to change despite the quantum yield differences between Wtyp and W32X mutants. In contrast to the situation with equimolar mixtures, it is unclear how to constrain these sums for the Wtyp protein. Given that the fit for the Wtyp protein is better than for equimolar mixtures of the single-Trp mutants, it is clear that this approach does not help demonstrate Trp–Trp interactions in this particular protein, and was not pursued further.

TABLE 3A Linked decay analysis of W32Y and W220Y mutants with an equimolar mixture of the two proteins

	W32Y	W220Y	W32Y/W220Y mix
τ_1	6.09		linked
f_1	0.994		0.953
τ_2		3.94	linked
f_2		0.195	0.007
τ_3		0.51	linked
f_3		0.803	0.030
τ_4	0.42		linked
f_4	0.005		0.005
τ_5	0.03	linked	linked
f_5	0.002	linked	linked
χ^2	1.7	1.6	2.4

Similar results were obtained in two out of three measurements. In a third measurement, χ^2 values of 1.8, 2.0, and 2.1 were obtained with slight changes in the recovered parameter values. "Linked" indicates that the parameter was constrained to be equal for both proteins. The ratio f_1:f_4 in W32Y and the W32Y/W22-Y mixture was constrained to be equal, as was the ratio f_2:f_3 in W220Y and the W32Y/W22-Y mixture. The sum of $f_2 + f_3$ was held to 0.037 (the exact ratio of the quantum yields of W220Y and W32Y).

Acrylamide quenching

The susceptibility of these proteins to acrylamide quenching of their fluorescence was investigated using both lifetime and intensity measurements. The data were fit to three exponentials over all concentrations of acrylamide. However, with the exception of W220F, one component consistently emerged with a lifetime <0.055 ns and a fractional intensity of $<1\%$. As shown in Table 4, Trp fluorescence in all five proteins was quite resistant to quenching by acrylamide. Apparent bimolecular quenching constants (k_q) for the longest component in each protein ranged from $0.5–0.7 \cdot 10^9 M^{-1}s^{-1}$. In the Wtyp protein and both W32X mutants, the short component resisted quenching by up to 800 mM acrylamide,

TABLE 3B Linked decay analysis of W32Y and W220Y mutants with a Wtyp protein

	W32Y	W220Y	Wtyp
τ_1	6.11		linked
f_1	0.994		0.953
τ_2		3.95	linked
f_2		0.195	0.008
τ_3		0.51	linked
f_3		0.802	0.030
τ_4	0.37		linked
f_4	0.005		0.006
τ_5	0.03	linked	linked
f_5	0.002	linked	linked
χ^2	1.9	1.6	1.9

Similar results were obtained in two out of three measurements. In a third measurement, the fit would not converge with the same initial values given the other two fits, or the 3 fits described in Table 3*a*. Constraints are identical to that present in Table 3*a*.

TABLE 4 **Acrylamide quenching results for GlnBP and four mutants, reported as bimolecular quenching constants (k_q) in units of $10^9\ M^{-1}\ s^{-1}$**

Protein	Component	k_q	
		Lifetime-derived	Intensity-derived
Wtyp	τ_1	0.7	0.7
	τ_2	*	
W32Y	τ_1	0.7	0.9
	τ_2	ND	
W32F	τ_1	0.7	0.7
	τ_2	ND	
W220Y	τ_1	0.5	1.1
	τ_2	0.6	
	τ_3	ND	
W220F	τ_1	0.7	0.7
	τ_2	0.6	
	τ_3	ND	

For results derived from lifetime analysis, k_q is derived from the slope of $1/\tau$ versus [acrylamide] for acrylamide concentrations up to 200 mM (τ_1 and τ_2 refer to the lifetimes reported in Table 2). Protein concentrations were 20 μM and both set of measurements were performed in duplicate. *τ_2 was impervious to acrylamide concentrations as high as 1 M. Results derived from intensity measurements were linear over the range 0–700 mM acrylamide; the addition of 400 μM Gln did not have measurable consequences.

while the short component in the W220X mutants exhibited a $k_q = 0.5\text{–}0.6 \cdot 10^9 M^{-1}s^{-1}$. The use of intensity ratios to determine the quenching rates yielded essentially the same result for the Wtyp protein and W32X mutants, and the presence of 400 mM Gln had minor effects (data not shown).

DISCUSSION

The data suggest that the first decay component of the Wtyp protein arises almost entirely from Trp-220. They also suggest that W32Y more faithfully preserves those features of the wild-type environment which determine the lifetime of Trp-220 than does W32F (there is no overlap between the confidence interval of τ_1 for W32F and either W32Y or Wtyp). The origin of τ_2 in the Wtyp protein seems to be Trp-32, because a 0.4–0.5 ns component is recovered in both W220X mutants, and mixing a W220X mutant with a W32X mutant yields a 0.5-ns component as found in the Wtyp protein. However, the presence of additional components in the W220X mutants still leaves the precise origin of the shorter Wtyp component somewhat uncertain.

Are these results affected by Trp–Trp interactions in the Wtyp protein or by other factors related to Tyr or Phe substitution for Trp in the mutants? Earlier work by Shen et al. (9) has provided evidence for the overall structural integrity of the mutant proteins. First, within a factor of 2, all five proteins exhibit the same binding constant for Gln. Second, all five proteins function biologically to transport Gln, albeit with different transport activities. Third, the proton NMR spectral "fingerprints" in the region of low-field, exchangeable proton resonances are virtually superimposable.

However, the quantum yield data suggest that the photophysical environment of W220 in the W32X mutants differs from that of W220 in the Wtyp protein. The determination of relative quantum yield of Trp in a protein is problematic, both because of the extent to which photons are absorbed by other residues is unknown and because protein absorption spectra have particularly steep slopes in the vicinity of 295 nm, making the measurements sensitive to instrumental parameters such as slit width. Yet, our results are reproducible and indicate that the relative "molar" quantum yield (i.e., the photon yield per photon absorbed by a mole of protein) is higher in the single-Trp W32X mutants than in the Wtyp protein, despite twice as many Trp residues in the latter. Of note, these results are associated with another conspicuous feature of the W32X mutants: they lack an absorption shoulder at 293 nm (indicated by a negative second derivative in Fig. 1) which is present in the Wtyp and W220X proteins. Semiempirical quantum-mechanical calculations predict that a secondary absorption band exists at this wavelength and that electrostatic fields may alter the amplitude, shape, and position of such bands in indole and Trp (20). It is interesting to note that the ^{20}F-NMR results also suggest that the environment of Trp-220 in the Wtyp protein is different from that in mutant GlnBPs (6).

We see quantum yield differences as well as spectral and decay-rate differences depending on whether Tyr or Phe substitutes for Trp in the W220X mutants. These differences lead us to reason that if the remaining Trp residue is sensitive to the difference between Tyr and Phe, it will likely be also affected by the substitution of either Tyr or Phe for Trp. This reasoning is supported by ^{20}F-NMR results indicating that Trp-32 and Trp-220 in the Wtyp protein experience small but different environmental changes upon L-Gln binding to GlnBP, and that ^{20}F resonances in the single-Trp mutants respond differently from those of the Wtyp protein (6).

It should not be surprising that multiple components are recovered in the single Trp mutants of GlnBP. One reason is that the ability to recover individual lifetime components from a mixture of substances with "known" decay characteristics may be impossible when the ratio of their lifetimes is close to 1 or when the relative intensities differ greatly (21). Another reason is that it is

distinctly uncommon for a single Trp residue in a protein to exhibit a monoexponential intensity decay (11, 22). Even one of the best examples, ribonuclease-T1 at pH 5.5, appears to have a small but reproducible short lifetime component upon detailed analysis (21). However, without data from single-Trp mutants, many observers would be tempted to attribute one of the two decay components recovered from the Wtyp protein to each of the two Trp residues known to be present. Our results suggest that this may be a simplified picture of the actual decay behavior.

Of course, there are trivial reasons for the existence of additional components in the single-Trp proteins. For example, they may be conformationally impure, i.e., partially misfolded or denatured. This would be of most concern in the W220-X proteins because an altered fold may well alter the conditions which so highly quench Trp-32; a very small fraction of protein sample could thereby give rise to a much larger fraction of the total fluorescence. In any case, whether conformationally pure or not, it is clear that mixtures of the single-Trp proteins yield a decay which is virtually indistinguishable from that of the Wtyp protein.

Whereas it may seem obvious in cases such as GlnBP that weak components will be "lost," and similar components may be indistinguishable, we are only beginning to understand the actual limits of resolvability for intensity decay analysis, and the fundamental bases for such limits. For example, we have examined the role of purely statistical noise in impeding recoveries by conducting simulations in which instrumental noise, light scattering, and uncertainty as to the true answer are not present. Although various kinds of noise undoubtedly compound so as to obscure components with small fractional intensities, in the case of GlnBP it is clear that statistical (Poisson) noise alone is sufficient to preclude their recovery. Poisson noise may be reduced by collecting much larger numbers of photons. James et al. (23, 24) have shown that various statistical analyses are unable to reveal the presence of lifetime distributions in certain kinds of synthetic data when only 20,000 counts are in the peak channel. Furthermore, they showed that some Gaussian distributions of lifetimes will analyze to yield two discrete lifetimes. We were constrained in this study of GlnBP with respect to number of counts in a peak channel because instrument-induced noise superceded statistical noise as a problem before we could accumulate more than 100,000–200,000 counts in a peak channel (data not shown).

The data plotted in Fig. 2 suggest that the recovered lifetimes are distributed about the two major components when three or four components are fit to the simulated data, even if the data are synthesized using four discrete lifetimes. The recovered values have exceedingly narrow distributions if only two components are fit to the data (data not shown). The shape of the distribution when two or more components approximate the same lifetime is a consequence of each component contributing a portion of the total fractional intensity. This illustrates that a distribution of lifetimes may be recovered from photon counting data despite the existence of truly discrete lifetimes (25), and that this phenomenon may be due to the presence of unresolved components or unavoidable statistical noise (further work in progress).

Our results point to the need for an explicit treatment of scattered light in data fitting procedures. Virtually every intensity decay that we report herein actually required an additional component to achieve the quality of fit reported herein. These components are recovered irrespective of whether small or short values are given to the fitting procedure as initial guesses. A better treatment of this systematic error might involve a single parameter representing scattered intensity, with the distribution of this intensity dictated by the form of the instrument response function (21).

We have also analyzed our data in terms of lifetime distributions, but we did not obtain compelling results. In general, the quality of fit to the data for a given number of parameters was either no better or was not as good as the fit obtained through discrete lifetime analysis. Without a physical model suggesting a specific basis for such distributions, we cannot justify such an analysis of these data. Of course, neither can we exclude the actual existence of such distributions, or distributions of a form that we have not considered.

Royer et al. (7) used both multifrequency phase fluorometry and photon counting in their study of the two tryptophans of *lac* repressor using single Trp mutant forms of the protein. However, using only the phase fluorometry data, they concluded that the wild-type *lac* repressor decay was a weighted linear combination of single-Trp mutant decays. Photon counting and phase fluorometry instruments yield comparable answers (10), but are subject to fundamentally different types of noise and the "resolvability" of either method is not well understood. In particular, phase fluorometry yields a relative paucity of data points compared to photon counting. This impairs the utility of statistical tests used to determine goodness of fit.

Our approach contrasts with Royer et al. (7) both in our use of the photon counting technique and in that we required the ratio of weighting factors used for linear combination analysis to match the ratio of molar quantum yields. With weighting factor ratios imposed in this way, we supposed that Trp–Trp interactions (electronically or structurally mediated) would be the most likely reason for an inability to fit the Wtyp protein with a

linear combination of two single-Trp mutant decays. Given our inference that some sort of Trp–Trp interaction does indeed occur in GlnBP (based on quantum yield data), we were surprised to find that the Wtyp protein could be better represented by a linear combination of single-Trp decays than could an equimolar mixture of the single-Trp mutants. Thus, the overall sensitivity of linear combination analysis and whether this approach can detect Trp–Trp interactions remains unknown.

We might have expected to recover the discrete lifetimes input to a protein mixture by linking the model parameters and simultaneously fitting the decay functions recorded from individual proteins and the mixtures. We find, however, that additional components may be forced into the model without significantly degrading the overall fit of the model to the data. In other words, the multidimensional χ^2 surface in this case has a shallow gradient and no local minimum in the vicinity of the "true" component. Thus, the models which arise from simultaneous fits with parameter linkages will have parameters which are weighted according the steepness of their gradient with respect to the chi-squared surface; those parameters which have shallow gradients will be relatively more distorted and/or more likely to be "lost."

Both Trp residues appear to be somewhat shielded from quenching by acrylamide. The highest bimolecular quenching constant observed in any of these proteins is about 1/10 of that expected for a fully accessible residue. This is consistent with the blue shift of the emission spectra relative to fully accessible Trp residues. Assuming that the long and short intensity decay components in the Wtyp arise primarily from Trp-220 and Trp-32, respectively, it is noteworthy that the short component of the Wtyp protein is not quenched, whereas it is quenched in the W220X mutants. It appears that the susceptibility of Trp-32 to acrylamide quenching is altered by substituting Tyr or Phe for Trp-220. A possible, albeit simplistic explanation might be that Trp-220 is physically interposed between Trp-32 and the protein exterior. This would be consistent with the apparently greater solvent-accessibility for Trp-220, the less blue-shifted emission spectrum relative to Trp-32, and with NMR evidence for greater solvent accessibility of Trp-220 (6). Quenching measurements based on steady-state intensity data are in good agreement with the intensity decay-based measurements in the Wtyp protein and W32X mutants.

These fluorescence data, combined with earlier NMR studies, offer a number of specific predictions concerning the structure of GlnBP. A crystal structure of this protein would be useful to verify these predictions, and to further our ability to interpret Trp fluorescence in terms of protein structure. For example, the presence of a phenolic hydroxyl group (Tyr vs. Phe) at either position has clear and different consequences on the fluorescence of Trp-32 and Trp-220; the structure may yield important clues as to how such chemical moieties mediate various photophysical effects.

Valuable comments on the manuscript were provided by Joe Beechem and Terry Therneau.

This work was supported by National Institutes of Health grants GM-25874 (to C. Ho) and GM-34847 (to F. G. Prendergast), and National Science Foundation grant DMB 88-16384 (to C. Ho). P. H. Axelsen is a Markey Scholar supported by the L. P. Markey Charitable Trust.

Received for publication 8 April 1991 and in final form 17 May 1991.

REFERENCES

1. Privat, J.-P., P. Wahl, J.-C. Auchet, and R. H. Pain. 1980. Time-resolved spectroscopy of tryptophanyl fluorescence of yeast 3-phosphoglycerate kinase. *Biophys. Chem.* 11:239–248.
2. Ross, J. B. A., C. J. Schmidt, and L. Brand. 1981. Time-resolved fluorescence of the two tryptophans in horse liver alcohol dehydrogenase. *Biochemistry.* 20:4369–4377.
3. Royer, C. A., P. Tauc, G. Herve, and J.-C. Brochon. 1987. Ligand binding and protein dynamics: a fluorescence depolarization study of aspartate transcarbamylase from *Escherichia coli. Biochemistry.* 26:6472–6478.
4. Merola, F., R. Rigler, A. Holmgren, and J.-C. Brochon. 1989. Picosecond tryptophan fluorescence of thioredoxin: evidence for discrete species in slow exchange. *Biochemistry.* 28:3383–3398.
5. Brochon, J.-C., P. Wahl, M. Charlier, J. C. Maurizat, and C. Helene. 1977. Time-resolved spectroscopy of the tryptophanyl fluorescence of the *E. coli* lac repressor. *Biochem. Biophys. Res. Commun.* 79:1261–1271.
6. Shen, Q., V. Simplaceanu, P. F. Cottam, J.-L. Wu, J.-S. Hong, and C. Ho. 1989. Molecular, genetic, biochemical, and nuclear magnetic resonance studies on the role of tryptophan residues of glutamine-binding protein from *E. coli. J. Mol. Biol.* 210:859–867.
7. Royer, C. A., J. A. Gardner, J. M. Beechem, J.-C. Brochon, and K. S. Matthews. 1990. Resolution of the fluorescence decay of the two tryptophan residues of *lac* repressor using single tryptophan mutants. *Biophys. J.* 58:363–378.
8. Longworth, J. W. 1971. Luminescence of polypeptides and proteins. *In* Excited States of Proteins and Nucleic Acids. R. F. Steiner, and I. Weinryb, editors. Plenum Publishing Corp., New York.
9. Shen, Q., V. Simplaceanu, P. F. Cottam, and C. Ho. 1989. Proton nuclear magnetic resonance studies on glutamine-binding protein from *E. coli. J. Mol. Biol.* 210:849–857.
10. Hedstrom, J., S. Sedarous, and F. G. Prendergast. 1988. Measurements of fluorescence lifetimes by use of a hybrid time-correlated and multifrequency phase fluorometry. *Biochemistry.* 27:6203–6208.
11. Grinvald, A., and I. Z. Stenberg. 1976. The fluorescence decay of

tryptophan residues in native and denatured proteins. *Biochim. Biophys. Acta.* 427:663–678.

12. Press, W. H., B. P. Flannery, S. A. Teukolsky, and W. T. Vetterling. 1986. Numerical recipes, the art of scientific computing. Cambridge University Press, New York.
13. Knutson, J. R., J. M. Beechem, and L. Brand. 1983. Simultaneous analysis of multiple fluorescence decay curves: a global approach. *Chem. Phys. Lett.* 102:501–507.
14. Beechem, J. M., J. R. Knutson, J. B. A. Ross, B. W. Turner, and L. Brand. 1983. Global resolution of heterogenous decay by phase/modulation fluorometry: mixtures and proteins. *Biochemistry.* 22:6054–6058.
15. Beechem, J. M., and E. Gratton. 1988. Fluorescence spectroscopy data analysis environment: a second generation global analysis program. *Proc. Soc. Photoopt. Instr. Eng.* 909:70–81.
16. Beechem, J. M., E. Gratton, M. A. Ameloot, J. R. Knutson, and L. Brand. 1989. The global analysis of fluorescence intensity and anisotropy decay: second generation theory and programs. *In* Fluorescence Spectroscopy. Vol. I. Principles and Techniques. J. R. Lakowicz, editor. Plenum Publishing Corp., New York. In press.
17. Bevington, P. R. 1969. Data Reduction and Error Analysis for the Physical Sciences. McGraw-Hill, New York.
18. Weiner, J. H., and L. A. Heppel. 1971. A binding protein for glutamine and its relation to active transport in *E. coli. J. Biol. Chem.* 246:6933–6941.
19. Alcala, J. R., E. Gratton, and F. G. Prendergast. 1987. Fluorescence lifetime distributions in proteins. *Biophys. J.* 51:597–604.
20. Ilich, P., P. H. Axelsen, and F. G. Prendergast. 1988. Electronic transitions in molecules in static external fields I. Indole and Trp-59 in ribonuclease-T1. *Biophys. Chem.* 29:341–349.
21. Bajzer, Ž., and F. G. Prendergast. 1991. Maximum likelihood analysis of fluorescence data. *Methods Enzymol.* In press.
22. Beechem, J. M., and L. Brand. 1985. Time-resolved fluorescence of proteins. *Annu. Rev. Biochem.* 54:43–71.
23. James, D. R., Y.-S. Liu, P. De Mayo, and W. R. Ware. 1985. Distributions of fluorescence lifetimes: consequences for the photophysics of molecules adsorbed on surfaces. *Chem. Phys. Lett.* 120:460–465.
24. James, D. R., and W. R. Ware. 1986. Recovery of underlying distributions of lifetimes from fluorescence decay data. *Chem. Phys. Lett.* 126:7–11.
25. Siemiarczuk, A., B. D. Wagner, and W. R. Ware. 1990. Comparison of the maximum entropy and exponential series methods for the recovery of distributions of lifetimes from fluorescence data. *J. Phys. Chem.* 94:1661–1666.